Inorganica Chimica Acta 543 (2022) 121153

Contents lists available at ScienceDirect

Inorganica Chimica Acta

journal homepage: www.elsevier.com/locate/ica

Hydrogen bond-directed coordination of phosphine-amino-alcohol (P,N,OH) ligands: Stereochemical considerations and catalytic studies

Zsófia Császár [a], Mária Guóth [a], Evelin Farsang [b], Attila C. Bényei [c], József Bakos [a], Gergely Farkas [a,*]

[a] Research Group of Organic Chemistry – Synthesis and Catalysis, University of Pannonia, Egyetem u. 10, H-8200 Veszprém, Hungary
[b] Research Group of Analytical Chemistry, University of Pannonia, Egyetem u. 10, H-8200 Veszprém, Hungary
[c] Department of Physical Chemistry, University of Debrecen, Egyetem tér 1, H-4032 Debrecen, Hungary

ARTICLE INFO

Keywords:
Chiral P,N,OH ligand
Palladium
Allylic alkylation
Hydrogen bond

ABSTRACT

Novel phosphine-aminoalcohol type chiral ligands of the chemical formula $Ph_2PCH(CH_3)CH_2CH(CH_3)NHCH(R)CH_2OH$ (**1a**: (*R*,*R*)-(*S*), R = CH_3, **1b**: (*S*,*S*)-(*S*), R = CH_3, **1c**: (*S*,*S*), R = H) have been synthesized in two simple steps using cyclic sulfates. The coordination behavior of **1a-c** having stereochemically labile nitrogen donor to square planar Pd(II) center was investigated by X-ray crystallography, 1D and 2D NMR methods and by DFT calculations. In the solid state of complex [Pd(**1a**)Cl_2] an intramolecular hydrogen bond could be observed between the OH-moiety and one of the Cl co-ligands, while intermolecular hydrogen bonds were detected in the case of [Pd(**1b**)Cl_2] between the same functionalities. In the dichloromethane solution of the complexes the hydrogen bond was identified as a crucial factor in determining ring conformation and nitrogen configuration. Ligand **1a** coordinated stereoselectively to the metal in [Pd(**1a**)Cl_2] leading to a complex having a single conformationally rigid six-membered chelate and a configurationally fixed *N*-donor. In contrast, coordination of ligands **1b-c** resulted in the formation of a mixture of isomers with different chelate conformation and nitrogen configuration. The ligands were utilized in Pd-catalyzed asymmetric allylic alkylation where high enantioselectivities (*ees* up to 96 %) and activities could be obtained.

1. Introduction

A challenging direction of research in asymmetric catalysis is the design of new transition metal species that are composed of metal–ligand assemblies with meta-stable stereochemistry, i.e. the ligand structure is maintained in a specific spatial arrangement solely due to metal coordination. [1,2] In this respect, chiral ligands with non-persistent donoratom chirality (eg. ligands with non-symmetrically substituted sp^3 N- [3,4] or S-donors [5,6] represent a valuable class of compounds. In these cases, the stereoselective coordination of the corresponding donoratom ensures the efficient transfer of chirality from the catalyst to the substrate owing to the fact that the stereogenic center is directly connected to the metal. [7–17] Furthermore, by using this strategy, the rather tedious and complicated synthesis of optically pure ligands with configurationally stable donoratom(s) (eg. P-chiral compounds [18,19] can be avoided. It is, however, important to note that successful control over the stereoselectivity of the complexation requires the thorough understanding of the factors influencing the coordination and demands a modular synthetic approach that ensures the possibility of the careful structural fine tuning of the ligands. [20,11]

In addition to the stereoselective coordination, secondary interactions in the catalytically active species may further enhance the effectiveness of the chiral induction by influencing the conformation of the catalyst or by directing the attack/orientation of the reactants. [21] In a number of instances, a properly positioned hydroxyl function has been interpreted to have a dominating role in obtaining increased activity and/or enantioselectivity. An early example of such effects was observed by Knowles et al. when the substitution of the *ortho* methoxy-substituents of (*R*,*R*)-DIPAMP ((*R*,*R*-1,2-ethanediylbis[(2-methoxyphenyl)-phenylphosphine]) by hydroxyl-groups led to highly efficient Rh-catalyst. [22] Later, Börner reported on the unique effects of internal hydroxyl functions in chiral rhodium(I)-diphosphine catalysts on the asymmetric hydrogenation of functionalized olefins. These effects were attributed to the fact that the OH-group can coordinate to the metal exhibiting hemilabile behavior or to its ability to establish hydrogen bonding within the framework of the ligand or between the ligand and

* Corresponding author.
E-mail address: gerifarkas@almos.uni-pannon.hu (G. Farkas).

https://doi.org/10.1016/j.ica.2022.121153
Received 19 May 2022; Received in revised form 26 July 2022; Accepted 11 August 2022
Available online 13 August 2022

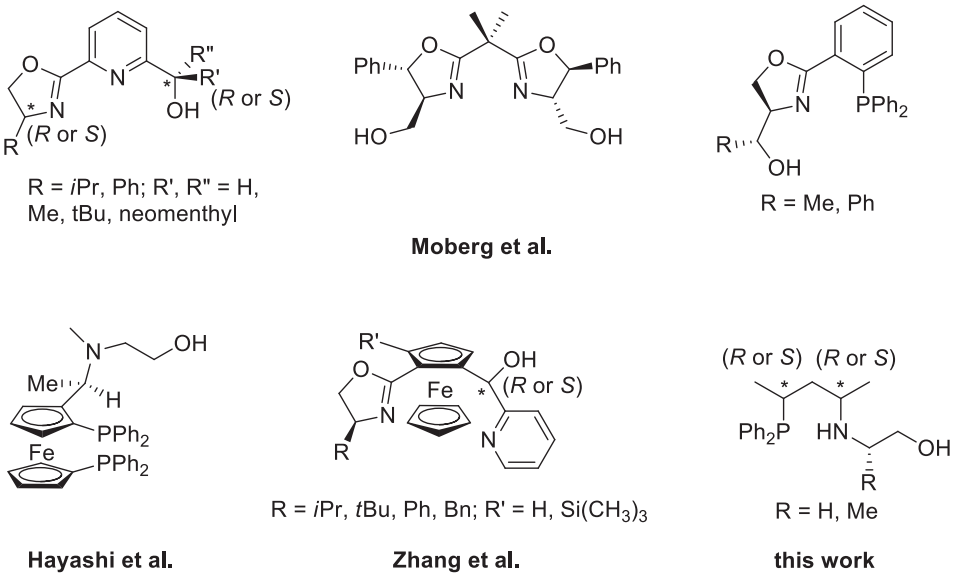

Fig. 1. Hydroxyl-containing chiral ligands used in Pd-catalyzed allylic alkylation reactions.

the substrate. [23]

Besides Rh-catalyzed asymmetric hydrogenation, Pd-catalyzed asymmetric allylic alkylation provides a convenient way to study the role of inter- and intramolecular hydrogen bonds in determining catalytic activity and selectivity. Furthermore, the presence of H-bond interactions, in many cases, has a beneficial effect in the catalytic process. Hayashi et al. developed a series of ferrocene based chiral diphosphines containing a pendant hydroxyalkyl sidearm (Fig. 1). [24] The ligands provided excellent enantioselectivities in palladium-catalyzed asymmetric allylic amination reactions that was partly ascribed to the selective nucleophilic attack of amine at one of the stereogenic allylic carbon atoms which was directed by the hydroxy group of the pendant side arm.

Moberg and coworkers found that in the Pd(0)-complexes of 2-(1-hydroxyalkyl)pyridinooxazoline, [25–26] hydroxyalkyl substituted *bis* (oxazoline) [27] or phosphino-4-(1-hydroxyalkyl)oxazoline [28] ligands (Fig. 1) a hydrogen bond between the metal and the hydroxyalkyl side group strongly influences the conformational preferences of the complex. This phenomenon was found to be a crucial factor in determining both the activity and the enantioselectivity in asymmetric allylic alkylation reactions.

Zhang et al. could achieve high enantioselectivities in asymmetric allylic alkylation by using OH-containing ferrocene-based oxazoline-pyridine type chiral ligands (Fig. 1). [29] The remarkable catalytic performance was attributed to an intramolecular hydrogen bond between the OH functionality and oxazoline moiety of the chiral ligand that affected the conformation of the catalyst.

Recently, we have found that pentane-2,4-diyl based chiral P,N-ligands [30] with stereogenic N-donor are capable of stereoselectively coordinate to Pd(II)-center resulting in the formation of Pd-catalysts with a conformationally rigid chelate having a configurationally fixed nitrogen and electronically different coordination sites due to presence of P and N donors (Fig. 1). [11] Inspired by our findings and the above literature results we decided to synthesize chiral alkane-diyl based P,N-ligands having N-(hydroxyalkyl) substituent in order to investigate their coordination chemistry and catalytic features in allylic alkylation reactions. Our primary aim was to exploit their advantageous features provided by (i) the high modularity of the synthetic procedure available for their preparation, (ii) the stereoselective coordination of the sp^3 N-atom, (iii) the stereoelectronic differentiation enabled by the P- and N-donors and (iv) the possibility of the formation of intramolecular hydrogen bonds, beneficial for the catalytic process.

2. Experimental

2.1. General experimental details

All manipulations were carried out under argon using Schlenk techniques. Solvents were purified, dried and deoxygenated by standard methods. All other starting materials were purchased from Sigma Aldrich and used without further purification. $^{31}P\{^1H\}$-, $^{13}C\{^1H\}$- and ^1H NMR measurements were carried out on a Bruker Avance 400 spectrometer (NMR Laboratory, University of Pannonia) operating at 161.98, 100.61 and 400.13 MHz respectively. The ^1H NMR and ^{13}C NMR signals were assigned from their related ^1H–^1H COSY and ^{13}C–^1H HSQC spectra, respectively (NMR Laboratory, University of Pannonia). X-ray data for compound **2a** and **2b** were recorded on a Bruker D8 Venture diffractometer. EI and ESI mass spectra were recorded on a Shimadzu GCMS QP2010 SE or on a Shimadzu LCMS-2020 spectrometer (Research Group of Analytical Chemistry, University of Pannonia), respectively. HPLC analysis was performed using a Hewlett Packard Series 1050 instrument. The details of X-ray characterization and DFT calculations are presented in the Supplementary Information.

2.2. Synthesis and characterization of the ligands

2.2.1. (2R,4R)-4-(Diphenylphosphino)-N-((S)-1-hydroxypropan-2-yl) pentan-2-amine (1a)

The (*S*)-2-amino-1-propanol (455 μL, 5.84 mmol) was added to the solution of (4*S*,6*S*)-4,6-dimethyl-1,3,2-dioxathiane 2,2-dioxide (970 mg, 5.84 mmol) in THF (3 mL) and the mixture was stirred for 48 h at room temperature. Next, ether (20 mL) was added to the mixture. The suspension formed was stirred for 30 min and filtered. The solid was washed two times with ether, the residual solvent was evaporated by vacuum to give (2*S*,4*R*)-4-(((*S*)-1-hydroxypropan-2-yl)ammonio)pentan-2-yl sulfate as a white powder. Yield: 62 %. ^1H NMR (400 MHz, DMSO-d_6): δ = 8.08 (broad s, 1H), 5.33 (broad s, 1H), 4.32 – 4.21 (m, 1H), 3.58 (dd, J = 11.6, 4.0 Hz, 1H), 3.52 – 3.42 (m, 3H), 1.85 – 1.77 (m, 1H), 1.53 (ddd, J = 14.1, 8.7, 2.2 Hz, 1H), 1.26 (d, J = 6.5 Hz, 3H, CH_3), 1.20 (d, J = 6.2 Hz, 3H, CH_3), 1.16 (d, J = 6.6 Hz, 3H, CH_3) ppm. ^{13}C NMR (101 MHz, DMSO-d_6): δ = 69.86 (s), 61.37 (s), 51.74 (s), 48.96 (s), 40.01 (s), 21.96 (s), 16.73 (s), 14.03 (s) ppm. $LiPPh_2$1,4-dioxane adduct (4.9 g, 17.61 mmol) was dissolved in THF (35 mL) under argon and the solution was cooled to 0 °C. (2*S*,4*R*)-4-(((*S*)-1-hydroxypropan-2-yl) ammonio)pentan-2-yl sulfate (850 mg, 3.52 mmol) was added to the red

solution in small portions. The reaction mixture was stirred at room temperature for 48 h. The color of the reaction mixture remained red. After evaporation of the solvent, deoxygenated water (60 mL) and ether (40 mL) were added to the residue and the mixture was stirred until the two phases became clear solutions. The pH of the mixture was then adjusted to 1 with 10 % deoxygenated HCl solution. The two phases were separated and the water phase was washed three times with 40 mL portions of ether. The pH was adjusted to about 9–10 with dropwise addition of a dilute solution of Na_2CO_3. The product was extracted four times with 40 mL portions of ether. After drying with $MgSO_4$ the solvent was evaporated. The crude product mixture was purified by column chromatography (silica gel, eluent: $CHCl_3$/MeOH 8/1) to give (2*R*,4*R*)-4-(diphenylphosphino)-N-((*S*)-1-hydroxypropan-2-yl)pentan-2-amine (**1a**) as a transparent oil. Yield: 82 %. ^{1}H NMR (400 MHz, $CDCl_3$): δ = 7.57 – 7.47 (m, 4H, aromatic), 7.41 – 7.30 (m, 6H, aromatic), 3.56 (dd, J = 10.7, 3.9 Hz, 1H, diast. C*H*H), 3.24 (dd, J = 10.7, 6.4 Hz, 1H, diast. CH*H*), 3.02 – 2.91 (m, 1H, CH), 2.85 (pd, J = 6.5, 4.0 Hz, 1H, CH), 2.53 (very broad s, 1H, OH), 2.51 – 2.38 (m, 1H, CH), 1.60 – 1.49 (m, 1H, diast. C*H*H), 1.43 – 1.31 (m, 1H, diast. CH*H*), 1.09 (d, J = 6.3 Hz, 3H, CH_3), 1.06 (dd, J = 14.7, 6.8 Hz, 3H, CH_3), 1.06 (d, J = 6.5 Hz, 3H, CH_3) ppm. ^{13}C NMR (101 MHz, $CDCl_3$): δ = 137.00 (d, J = 4.3 Hz, aromatic), 136.86 (d, J = 5.6 Hz, aromatic), 133.75 (d, J = 19.4 Hz, aromatic), 133.52 (d, J = 18.8 Hz, aromatic), 128.79 (s, aromatic), 128.72 (s, aromatic), 128.37 (d, J = 7.0 Hz, aromatic), 128.28 (d, J = 7.2 Hz, aromatic), 65.30 (s), 51.62 (s), 48.51 (d, J = 11.9 Hz), 40.72 (d, J = 16.2 Hz), 27.36 (d, J = 10.0 Hz), 20.88 (s), 17.92 (s), 16.42 (d, J = 15.5 Hz) ppm. ^{31}P NMR (162 MHz, $CDCl_3$): δ = -1.32 (s) ppm. MS (EI) *m/z* calculated for $C_{20}H_{28}NOP$ [M^+] 329.19, found: 329.

2.2.2. (2S,4S)-4-(Diphenylphosphino)-N-((S)-1-hydroxypropan-2-yl) pentan-2-amine (1b)

Compound **1b** was synthesized according to the procedure described for **1a**. The corresponding intermediate (2*R*,4*S*)-4-(((*S*)-1-hydroxypropan-2-yl)ammonio)pentan-2-yl sulfate was prepared as a white powder. Yield: 63 %. ^{1}H NMR (400 MHz, DMSO-d_6): δ = 8.05 (broad s, 1H), 5.34 (broad s, 1H), 4.34 – 4.24 (m, 1H), 3.61 – 3.55 (m, 1H), 3.51 – 3.42 (m, 1H), 1.91 – 1.82 (m, 1H), 1.59 (dd, J = 12.6, 8.4 Hz, 1H), 1.23 (d, J = 6.0 Hz, 3H, CH_3), 1.20 (d, J = 5.9 Hz, 3H, CH_3), 1.15 (d, J = 6.0 Hz, 3H, CH_3) ppm. ^{13}C{^{1}H} NMR (101 MHz, DMSO-d_6): δ = 70.27 (s), 61.58 (s), 51.90 (s), 48.97 (s), 40.34 (s), 22.06 (s), 15.96 (s), 13.10 (s) ppm. The title compound (2*S*,4*S*)-4-(diphenylphosphino)-N-((*S*)-1-hydroxypropan-2-yl)pentan-2-amine (**1b**) is a transparent oil. Yield: 78 %. ^{1}H NMR (400 MHz, $CDCl_3$): δ = 7.60 – 7.46 (m, 4H, aromatic), 7.42 – 7.29 (m, 6H, aromatic), 3.54 (dd, J = 10.7, 4.1 Hz, 1H, diast. C*H*H), 3.23 (dd, J = 10.7, 7.2 Hz, 1H, diast. CH*H*), 3.04 – 2.93 (m, 1H, CH), 2.93 – 2.82 (m, 1H, CH), 2.75 (very broad s, 1H, OH), 2.51 – 2.38 (m, 1H, CH), 1.59 – 1.36 (m, 2H, CH_2), 1.07 (dd, J = 14.8, 6.8 Hz, 3H, CH_3), 1.06 (d, J = 6.2 Hz, 3H, CH_3), 1.04 (d, J = 6.5 Hz, 3H, CH_3) ppm. ^{13}C NMR (101 MHz, $CDCl_3$): δ = 136.97 (d, J = 10.6 Hz, aromatic), 136.83 (d, J = 11.5 Hz, aromatic), 133.85 (d, J = 19.4 Hz, aromatic), 133.63 (d, J = 19.0 Hz, aromatic), 128.92 (s, aromatic), 128.89 (s, aromatic), 128.51 (d, J = 7.0 Hz, aromatic), 128.41 (d, J = 7.2 Hz, aromatic), 65.66 (s), 51.86 (s), 48.45 (d, J = 12.4 Hz), 41.26 (d, J = 17.3 Hz), 27.30 (d, J = 10.2 Hz), 19.86 (s), 17.31 (s), 16.46 (d, J = 15.3 Hz) ppm. ^{31}P NMR (162 MHz, $CDCl_3$): δ = -0.41 (s) ppm. MS (EI) *m/z* calculated for $C_{20}H_{28}NOP$ [M^+] 329.19, found: 329.

2.2.3. (2S,4S)-4-(Diphenylphosphino)-N-(2-hydroxyethyl)pentan-2-amine (1c)

Compound **1c** was synthesized according to the procedure described for **1a**. The corresponding intermediate (2*R*,4*S*)-4-((2-hydroxyethyl) ammonio)pentan-2-yl sulfate was prepared as a white powder. Yield: 74 %. ^{1}H NMR (400 MHz, DMSO-d_6): δ = 5.20 (broad s, 1H), 4.33 – 4.24 (m, 1H), 3.63 (t, J = 5.3 Hz, 2H), 3.42 – 3.32 (m, 1H), 3.03 – 2.88 (m, 2H), 1.88 – 1.78 (m, 1H), 1.55 (ddd, J = 14.2, 8.1, 2.2 Hz, 1H), 1.23 (d, J = 6.5 Hz, 3H, CH_3), 1.20 (d, J = 6.2 Hz, 3H, CH_3) ppm. ^{13}C{^{1}H} NMR (101 MHz, DMSO-d_6): δ = 70.34 (s), 56.77 (s), 51.62 (s), 45.53 (s), 39.73 (s), 22.02 (s), 16.02 (s) ppm. The title compound (2*S*,4*S*)-4-(diphenylphosphino)-N-(2-hydroxyethyl)pentan-2-amine (**1c**) is a transparent oil. Yield: 67 %. ^{1}H NMR (400 MHz, $CDCl_3$): δ = 7.53 – 7.43 (m, 4H, aromatic), 7.35 – 7.25 (m, 6H, aromatic), 3.61 – 3.53 (m, 2H, CH_2), 2.86 – 2.79 (m, 1H, CH), 2.77 – 2.70 (m, 1H, diast. C*H*H), 2.70 – 2.62 (m, 1H, diast. CH*H*), 2.57 (broad s, 1H, OH), 2.47 – 2.35 (m, 1H, CH), 1.57 – 1.45 (m, 1H, diast. C*H*H), 1.43 – 1.32 (m, 1H, diast. CH*H*), 1.03 (d, J = 6.3 Hz, 3H, CH_3), 1.02 (dd, J = 14.8, 6.9 Hz, 3H, CH_3) ppm. ^{13}C NMR (101 MHz, $CDCl_3$): δ = 136.98 (d, J = 2.8 Hz, 1C, aromatic), 136.84 (d, J = 3.9 Hz, 1C, aromatic), 133.73 (d, J = 19.3 Hz, 2C, aromatic), 133.54 (d, J = 19.0 Hz, 2C, aromatic), 128.77 (s, 2C, aromatic), 128.39 (d, J = 7.0 Hz, 2C, aromatic), 128.29 (d, J = 7.1 Hz, 2C, aromatic), 60.86 (s, 1C), 50.95 (d, J = 11.9 Hz, 1C), 48.18 (s, 1C), 40.46 (d, J = 16.8 Hz, 1C), 27.24 (d, J = 10.0 Hz, 1C), 19.72 (s, 1C), 16.42 (d, J = 15.6 Hz, 1C) ppm. ^{31}P NMR (162 MHz, $CDCl_3$): δ = -0.67 (s) ppm. MS (EI) *m/z* calculated for $C_{19}H_{26}NOP$ [M^+] 315.18, found: 315.

2.3. Synthesis and characterization of Pd-complexes

2.3.1. [Pd(1a)Cl$_2$] (2a)

Ligand **1a** (57.7 mg, 0.175 mmol) dissolved in CH_2Cl_2 (5 mL) was added dropwise to a solution of [Pd(COD)Cl_2] (50 mg, 0.175 mmol) in CH_2Cl_2 (5 mL). (COD: *Z,Z*-cycloocta-1,5-diene.) The resulting yellow solution was stirred for 3 h, filtered through a short pad of Celite and concentrated to *ca.* 2 mL. The solution was then treated with ether (10 mL) to precipitate a yellow powder that was filtered and washed with ether (3 × 5 mL) to give **2a**. Yield: 89 %. ^{1}H NMR (400 MHz, CD_2Cl_2): δ = 8.14 – 8.07 (m, 2H, aromatic), 7.71 – 7.64 (m, 1H, aromatic), 7.64 – 7.57 (m, 2H, aromatic), 7.52 – 7.46 (m, 1H, aromatic), 7.43 – 7.34 (m, 4H, aromatic), 4.83 (d, J = 13.0 Hz, 1H, diast. C*H*HO), 4.30 (d, J = 12.4 Hz, 1H, NH), 3.80 (broad s, 1H, OH), 3.23 – 3.11 (m, 2H, CHN and diast. CH*H*O), 2.75 – 2.62 (m, 1H, CHP), 2.42 – 2.32 (m, 1H, C*H*CH_2O), 2.20 (dddd, J = 15.9, 13.1, 8.1, 2.8 Hz, 1H, diast. C*H*H), 2.00 (dddt, J = 35.1, 15.8, 3.4, 3.4, 1.0 Hz, 1H, diast. CH*H*), 1.87 (d, J = 6.5 Hz, 3H, C*H*$_3$CHN), 1.21 (dd, J = 12.7, 7.2 Hz, 3H, C*H*$_3$CHP), 1.11 (d, J = 6.5 Hz, 3H, CH_3) ppm. ^{13}C NMR (101 MHz, CD_2Cl_2): δ = 134.35 (d, J = 9.6 Hz, 2C, aromatic), 133.01 (d, J = 9.7 Hz, 2C, aromatic), 132.62 (d, J = 2.8 Hz, 1C, aromatic), 131.17 (d, J = 3.1 Hz, 1C, aromatic), 129.73 (d, J = 10.6 Hz, 2C, aromatic), 128.32 (d, J = 64.0 Hz, 1C, aromatic), 128.29 (d, J = 11.9 Hz, 2C, aromatic), 124.81 (d, J = 47.0 Hz, 1C, aromatic), 65.42 (s, 1C, CH_2O), 56.85 (s, 1C, *C*HCH_2O), 48.75 (d, J = 3.7 Hz, 1C, CHN), 33.26 (s, 1C, CH_2), 24.73 (d, J = 27.5 Hz, 1C, CHP), 20.43 (s, 1C, *C*H$_3$CHN), 16.52 (d, J = 8.5 Hz, 1C, *C*H$_3$CHP), 15.17 (s, 1C, CH_3) ppm. ^{31}P NMR (162 MHz, CD_2Cl_2): δ = 23.85 (s) ppm. MS (ESI) *m/z* calculated for $C_{20}H_{28}ClNOPPd$ [M^+−Cl] 472.06, found: 472.

2.3.2. [Pd(1b)Cl$_2$] (2b)

The complex was synthesized according to the procedure described for compound [Pd(**1a**)Cl_2]. Yield: 85 %. *Isomer I*: ^{1}H NMR (400 MHz, CD_2Cl_2): δ = 8.12 – 7.42 (m, 10*H*, aromatic overlapped with the corresponding signals of isomer II), 7.19 (d, J = 7.3 Hz, 1H, NH), 4.28 (t, J = 10.7 Hz, 1H, diast. C*H*HO), 3.56 – 3.50 (m, 1H, diast. CH*H*O), 3.40 – 3.24 (m, 1H, C*H*CH_2O, overlapped with the next signal), 3.40 – 3.24 (m, 1H, CHN, overlapped with the previous signal), 2.49 – 2.37 (m, 1H, diast. C*H*H), 2.36 – 2.26 (m, 1H, CHP), 2.06 – 1.90 (m, 1H, diast. CH*H*, partially overlapped with the corresponding signal of isomer II), 1.28 (d, J = 6.3 Hz, 3H, C*H*$_3$CHN), 1.22 (d, J = 6.3 Hz, 3H, CH_3), 0.98 (dd, J = 13.7, 6.7 Hz, 3H, C*H*$_3$CHP) ppm. ^{13}C NMR (101 MHz, CD_2Cl_2): δ = 135.73 – 125.58 (12C, aromatic, together with the corresponding signals of isomer II), 69.57 (s, 1C, CH_2O), 59.72 (s, 1C, *C*HCH_2O), 48.76 (s, 1C, CHN), 40.62 (d, J = 6.2 Hz, 1C, CH_2), 21.42 (d, J = 30.1 Hz, 1C, CHP), 17.46 (s, 1C, *C*H$_3$CHN), 16.93 (d, J = 6.3 Hz, 1C, CH_3CHP), 11.99 (s, 1C, CH_3) ppm. ^{31}P NMR (162 MHz, CD_2Cl_2): δ = 29.23 (br s) ppm. *Isomer II*: ^{1}H NMR (400 MHz, CD_2Cl_2): δ = 8.12 – 7.42 (m, 10*H*, aromatic overlapped with the corresponding signals of isomer I), 5.73 (s, 1H, NH),

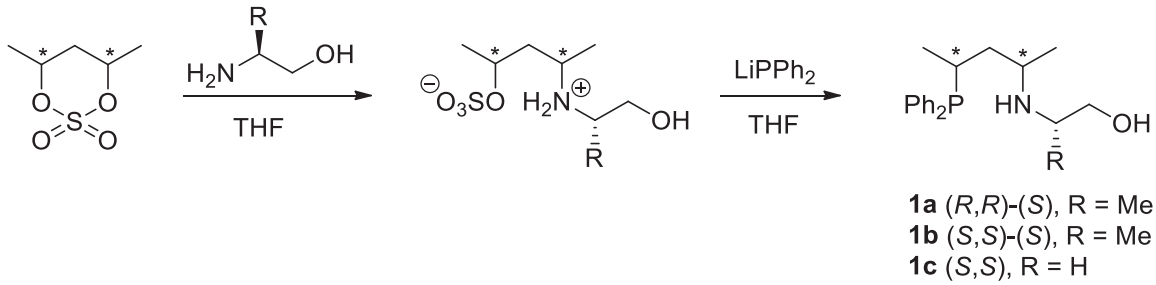

Fig. 2. Two-step synthesis of chiral ligands **1a-c.**

4.00 (d, $J = 12.2$ Hz, 1H, diast. C*H*HO), 3.36 (d, $J = 11.2$ Hz, 1H, diast. CH*H*O, partially overlapped with the signals of isomer I), 3.23 – 3.15 (m, 1H, CHN), 2.91 – 2.74 (m, 1H, C*H*CH$_2$O), 2.75 – 2.62 (m, 1H, CHP), 2.23 – 2.09 (m, 1H, diast. C*H*H, partially overlapped with the next signal), 2.16 – 1.98 (m, 1H, diast. CH*H*, partially overlapped with the previous signal), 1.60 (d, $J = 6.4$ Hz, 3H, C*H*$_3$CHN), 1.42 (d, $J = 6.7$ Hz, 3H, CH$_3$), 1.08 (dd, $J = 14.0$, 7.2 Hz, 3H, C*H*$_3$CHP) ppm. ^{13}C NMR (101 MHz, CD_2Cl_2): $\delta = 135.73 – 125.58$ (12C, aromatic, together with the corresponding signals of isomer I), 64.61 (s, 1C, CH$_2$O), 56.55 (s, 1C, *C*HCH$_2$O), 49.52 (d, $J = 3.2$ Hz, 1C, CHN), 36.65 (s, 1C, CH$_2$), 24.77 (d, $J = 29.1$ Hz, 1C, CHP), 20.73 (s, 1C, *C*H$_3$CHN), 18.89 (s, 1C, CH$_3$), 16.61 (d, $J = 5.6$ Hz, *C*H$_3$CHP) ppm. ^{31}P NMR (162 MHz, CD_2Cl_2): $\delta = 26.66$ (s) ppm. MS (ESI) *m/z* calculated for $C_{20}H_{28}ClNOPPd$ [M$^+$−Cl] 472.06, found: 472.

2.3.3. [Pd(1c)Cl$_2$] (2c)

The complex was synthesized according to the procedure described for compound [Pd(**1a**)Cl$_2$]. Yield: 78 %. *Major isomer*: ^{1}H NMR (400 MHz, CD_2Cl_2): $\delta = 8.23 – 8.09$ (m, 2H, aromatic), 7.73 – 7.65 (m, 1H, aromatic), 7.66 – 7.58 (m, 2H, aromatic), 7.54 – 7.46 (m, 1H, aromatic), 7.45 – 7.36 (m, 4H, aromatic), 4.75 (s, 1H, NH), 4.40 (s, 1H, diast. C*H*HO), 3.84 (s, 1H, OH), 3.54 – 3.37 (m, 1H, diast. CH*H*), 3.08 – 2.89 (m, 1H, CHN), 2.82 – 2.62 (m, 1H, CHP), 2.48 – 2.36 (m, 2H, C*H*$_2$CH$_2$O), 2.30 – 2.18 (m, 1H, diast. C*H*H), 2.09 – 1.90 (m, 1H, diast. CH*H*), 1.79 (d, $J = 6.6$ Hz, 3H, C*H*$_3$CHN), 1.21 (dd, $J = 12.8$, 7.2 Hz, 3H, C*H*$_3$CHP) ppm. ^{13}C NMR (101 MHz, CD_2Cl_2): $\delta = 135.38$ (d, $J = 9.8$ Hz, 2C, aromatic), 133.40 (d, $J = 9.6$ Hz, 2C, aromatic), 133.22 (d, $J = 2.6$ Hz, 1C, aromatic), 131.65 (d, $J = 3.0$ Hz, 1C, aromatic), 130.16 (d, $J = 10.7$ Hz, 2C, aromatic), 128.81 (d, $J = 12.0$ Hz, 2C, aromatic), 128.68 (d, $J = 62.5$ Hz, 1C, aromatic), 124.93 (d, $J = 47.3$ Hz, 1C, aromatic), 59.53 (s, 1C, CH$_2$O), 56.43 (s, 1C, *C*H$_2$CH$_2$O), 55.28 (d, 1C, $J = 3.6$ Hz, CHN), 34.38 (s, 1C, CH$_2$), 24.65 (d, $J = 27.6$ Hz, 1C, CHP), 20.51 (s, *C*H$_3$CHN), 17.23 (d, $J = 8.3$ Hz, 1C, *C*H$_3$CHP) ppm. ^{31}P NMR (162 MHz, CD_2Cl_2): $\delta = 25.00$ (s) ppm. *Minor isomer*: ^{31}P NMR (162 MHz, CD_2Cl_2): $\delta = 28.47$ (s) ppm. MS (ESI) *m/z* calculated for $C_{19}H_{26}ClNOPPd$ [M$^+$−Cl] 456.05, found: 456.

2.4. Catalytic experiments

A degassed solution of [Pd(η^3-C$_3$H$_5$)Cl]$_2$ (2.28 mg, 0.00625 mmol) and chiral ligand (0.0125 mmol) in CH_2Cl_2 (10 mL) was stirred for 15 min, then the substrate (315 mg, 1.25 mmol) was added and the solution was stirred for a further 15 min. Subsequently, dimethyl malonate (0.43 mL, 3.75 mmol), potassium acetate (7 mg) and *N,O*-bis(trimethylsilyl)-acetamide (BSA, 0.91 mL, 3.75 mmol) were added and the reaction mixture was stirred at room temperature. After being stirred, it was diluted with ether (10 mL) and a saturated aqueous solution of NH_4Cl was added. The mixture was extracted with ether (3 × 10 mL) and the extract dried over $MgSO_4$. The solution was then passed through a short pad of silica and was eluted with ether. The solvent was then evaporated and the residue dissolved in a mixture of *n*-hexane/2-propanol. The enantioselectivity and the conversion were determined by chiral HPLC. HPLC separation conditions for (*E*)-dimethyl-2-(1,3-diphenylallyl) malonate: column: Kromasil 3-AmyCoat, eluent: *n*-hexane/2-propanol 85/15, $\lambda = 254$ nm, flow rate: 0.5 mL/min, t_R (*R*) = 10.8 min, t_R (*S*) = 14.4 min.

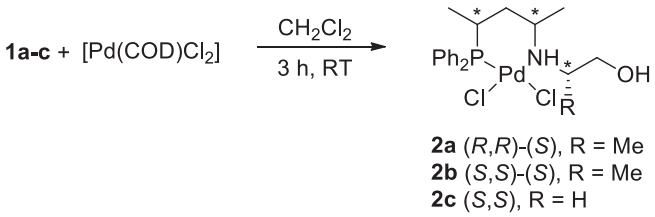

Fig. 3. Synthesis of Pd(II)-complexes of ligands **1a-c.**

3. Results and discussion

3.1. Synthesis of the novel ligands and their Pd(II)-complexes

The novel chiral P,N,OH ligands **1a-c** were synthesized in two simple steps (Fig. 2). First, the nucleophilic ring opening of the cyclic sulfate of optically pure pentane-2,4-diol by the corresponding aminoalcohol resulted in the formation of the sulfated amine in a zwitterionic form. In the next step, the addition of excess $LiPPh_2$ in THF provided the desired ligands in good yields after column chromatography. It is important to mention that both steps occur with complete inversion at the stereogenic centers, thus ligands **1a-c** exhibit one single line in their $^{31}P\{^1H\}$ NMR spectra. Additionally, the synthetic methodology is highly modular due

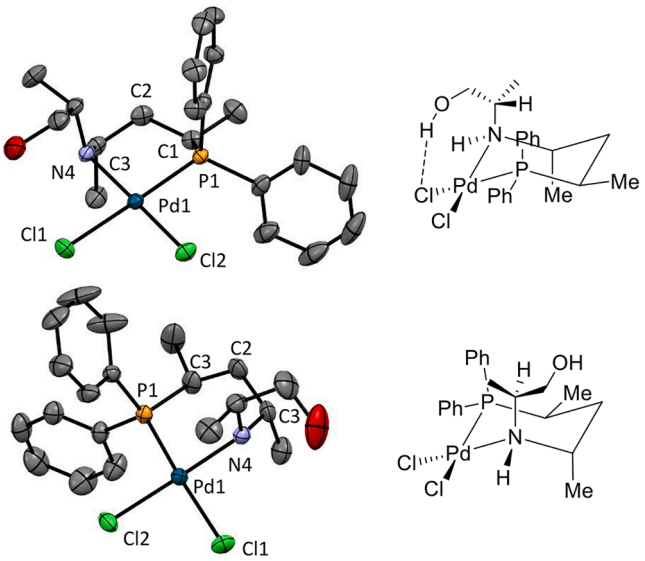

Fig. 4. ORTEP and schematic view of **2a** (top) and **2b** (bottom). (Hydrogen atoms are omitted for clarity, thermal ellipsoids are depicted at 30% probability level.)

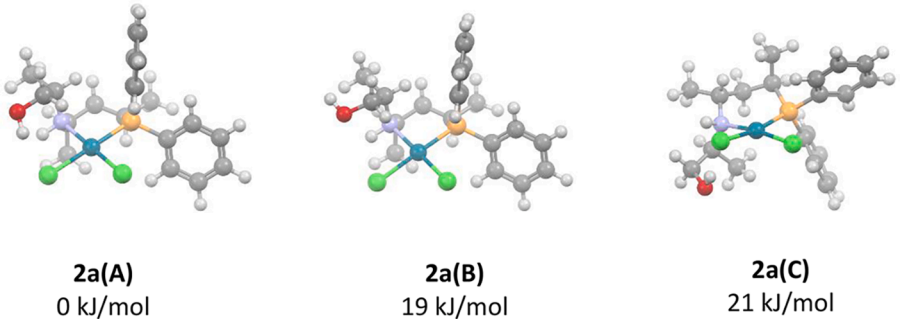

Fig. 5. Calculated conformational/configurational minima of **2a.**

to the structural versatility of the commercially available aminoalcohols and offers a convenient way of chiral ligand synthesis without tedious workup procedures.

In order to study the Pd(II) coordination chemistry of the ligands, complexes of the chemical composition [Pd(L)Cl_2] (**2a-c**) have been prepared in the reaction of **1a-c** and the suitably labile metal precursor, [Pd(COD)Cl_2] (Fig. 3) using dichloromethane as solvent.

3.2. Characterization of chiral Pd(II)-complexes

The Pd(II)-complexes of ligands **1a-c** have been characterized in CD_2Cl_2 solution by 1D and 2D NMR spectroscopy, and **2a** and **2b** in the solid phase by X-ray crystallography. In order to gain a deeper insight into the thermodynamic stability of the possible stereoisomers DFT structure optimization was also performed using the CAM-B3LYP functional combination with the SDD basis set and pseudopotential for Pd as well as the 6-31G* basis set for the rest of the atoms. Solvent effects of dichloromethane were taken into account using the CPCM implicit solvation model.

Single crystals of complexes **2a** and **2b** suitable for X-ray structure analysis were grown by the slow evaporation of the solvent from their solution in CH_2Cl_2. The solid phase structure of complex **2a** (Fig. 4) contains a six-membered chelate with a square planar Pd subunit having interatomic distances of 2.106(6) (Pd-N), 2.237(2) (Pd-P), 2.380(2) (Pd-Cl *trans* to P) and 2.296(2) Å (Pd-Cl *trans* to N) (for further geometric data see Table S2 in the SI). The six-membered chelate ring is stabilized in a chair conformation with equatorially and axially positioned ring substituents moving from the phosphorus towards the nitrogen along the ligand backbone. The nitrogen substituent is disposed in an axial position so that its CH proton points toward the center of the chelate ring. Thus, the nitrogen adopts (*R*) absolute configuration and the OH group of the *N*-side chain is directed towards the Cl-ligand *cis* to the N. The distance between the O and Cl atoms is 3.085(8) Å, and is within the sum of the van der Waals radius of the two atoms (3.27 Å). The close proximity of the two atoms strongly suggest the presence of an intramolecular OH…Cl type hydrogen bond.

The X-ray structure analysis of **2b** revealed that the complex is stabilized in the same six-membered chelate conformation, i.e. the methyl substituents of the backbone are in equatorial and axial positions, moving from the P to the N, respectively (Fig. 4). Furthermore, the *N*-substituent again occupies an axial position with its methine hydrogen pointing towards the center of the ring. As the two backbone chirality centers have opposite configurations compared to those of **2a**, but that of the *N*-substituent is the same (*S*), the coordinated nitrogen has (*S*)-configuration and the OH moiety is oriented away from the Cl ligand in this case resulting in an intramolecular O-Cl distance of 4.25 Å far away from a possible hydrogen bond. This spatial arrangement prevents the formation of an OH…Cl type intramolecular hydrogen bond, but certainly increases the possibility of intermolecular H-bonding. Indeed, in the unit cell of **2b** intermolecular OH…Cl interactions can be observed between the OH group of one molecule and a Cl ligand of a symmetry related complex *trans* to its nitrogen (Figure S3). The structures are also stabilized by weak C—H…Cl hydrogen bonds. These interactions link the molecules to line up into endless chains with intermolecular Pd-Pd distances of 7.1941(7) Å. A comparison of the OH…Cl type H-bond geometry in **2a** and **2b** suggests the intramolecular interaction in **2a** to be considerably stronger than the intermolecular bond in **2b**. This is most obvious from the much shorter intramolecular O-Cl distance in **2a** (3.085(8) Å) compared to the intermolecular distance (3.513(10) Å) between the corresponding O an Cl atoms in **2b**. A similar conclusion can be drawn from the O—H…Cl bond angle that is closer to linearity in **2a** (167°) than in **2b** (154°) (Table S3 and S5). [31]

The X-ray structures also provides information on the possible factors determining the preferred ring conformation. In both complexes the sterically demanding N-substituent and the adjacent Me-group of the backbone are *anti*-positioned relative to each other (1,2-diaxial arrangement) and the CH of the axial N-group points toward the center of the chelate thus minimizing steric congestion. The axial disposition of the N-substituent is also favoured due to the presence of the *cis* Cl co-ligand in the square planar palladium subunit. In this preferred arrangement, however, only complex **2a** is stabilized by intramolecular H-bond (Table S2 and S3).

In order to elucidate the solution phase structure of complexes **2a-c**, they were subjected to 1D and 2D NMR analysis using CD_2Cl_2 as solvent. The ^{1}H and $^{13}C\{^{1}H\}$ NMR spectra of the complexes were assigned with the help of COSY and HSQC techniques. Complex **2a** exists in solution as a single isomer. The detailed conformational analysis confirms in all respects the structural attributes deduced from the X-ray structure. [11] A nice indication of the axial position of the *N*-substituent is the characteristic W-coupling between one of the methylene hydrogens and the N—H (^{4}J(H,H) ~ 1 Hz), that is only possible when the latter is oriented equatorially. Furthermore, the large coupling (^{3}J(H,H) = 12.4 Hz) between the NH and the CH of the *N*-substituent suggests the CH pointing towards the center of the ring. These findings clearly evidence that the nitrogen coordinates stereoselectively with (*R*)-configuration and the six-membered chelate is fixed in one single chair conformation where the OH is directed towards the Cl-ligand enabling the formation of intramolecular H-bond.

Interestingly, the solution of **2b** in CD_2Cl_2 exhibits two major signals in its $^{31}P\{^{1}H\}$ NMR spectrum in a ratio of 1:1 and additional minor species (~10 % according to $^{31}P\{^{1}H\}$ NMR) can be detected at room temperature. The exact conformational analysis of the isomers could not be performed due to the significant overlapping of the ^{1}H NMR signals. Nevertheless, NMR spectroscopy clearly proved that unlike ligand **1a**, compound **1b** do not coordinate in a stereoselective manner giving rise to the formation of stereoisomers. A reasonable explanation for the non-stereoselective coordination is that in solution significant stabilization by intramolecular hydrogen bond may occur only in stereoisomers that are different from that observed in the solid phase.

In the $^{31}P\{^{1}H\}$ NMR spectrum of complex [Pd(**1c**)Cl_2] two signals appear in a ratio of 88/12 at room temperature. The major isomer has the same chelate conformation and N-configuration (*S*) as **2b** in the solid

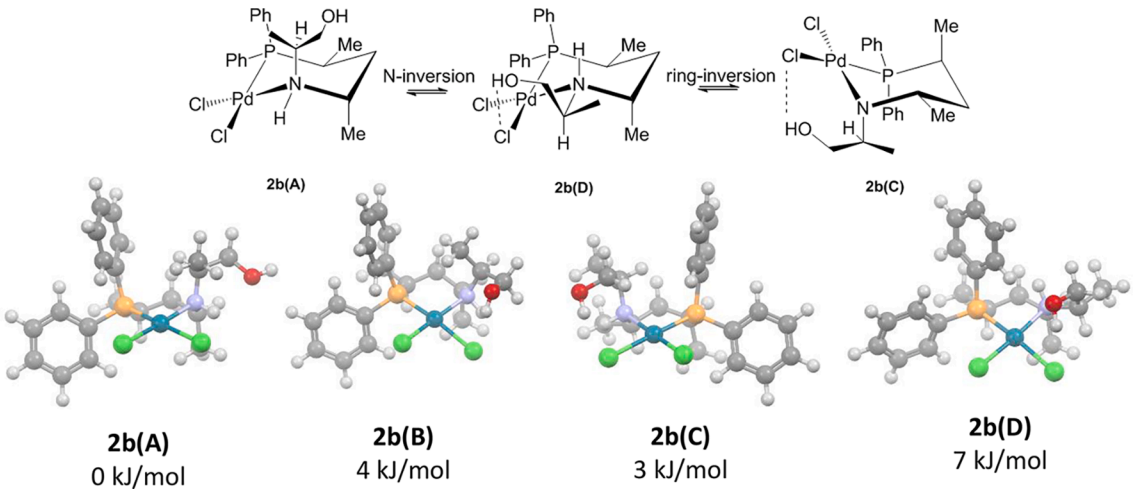

Fig. 6. Calculated conformational/configurational minima of **2b.**

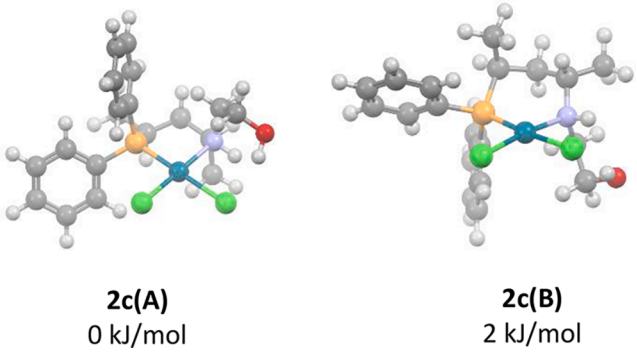

Fig. 7. Computed conformational/configurational minima of complex **2c.**

state according to its ^{1}H NMR spectrum. [11]

In order to determine the role of the intramolecular hydrogen bonding in the complex formation, DFT structures of different conformations have been calculated. At first, starting from the X-ray structure of complex **2a**, two conformational minima have been found when changing the C—C—O—H torsion angle (Fig. 5, 2a**(A)** and **2(B)**). **2a(A)** contains the OH-bond pointing towards the Cl co-ligand (C—C—O—H torsion angle: 92.25°), in **2a(B)** the hydrogen points in almost the opposite direction (C—C—O—H torsion angle: −78.45°). The enthalpy difference between the two structures (19 kJ/mol) evidences the significant stabilizing effect generated by the intramolecular hydrogen bond in **2a(A)**. The formation of the H-bond in **2a(A)** is also proved by its slightly elongated O—H bond (0.976 Å) compared to that in **2a(B)** (0.968 Å). Further possible chair conformers with different N-configuration were also calculated, but the stereoisomer corresponding to the X-ray structure having intramolecular H-bond proved to be the most stable at least by 21 kJ/mol relative to next energetically most favorable structure (**2a(C)**).

In contrast to these, the enthalpy differences between the isomers of **2b** with different chelate conformation and N-configuration are much smaller, that forecasts the appearance of more than one stereoisomers in solution (Fig. 6). Again, the most stable structure has the same ring conformation and nitrogen configuration as was found in the solid phase without intramolecular H-bond (**2b(A)**). Although the simple rotation of its *N*-substituent enables the formation of H-bond (**2b(B)**), it cannot fully compensate the unfavorable steric interactions in this ring conformation resulting in somewhat higher enthalpy. However, the nitrogen- and ring-inversion of this isomer produces a structure where the OH of the *N*-substituent will be directed towards the chloro-ligand *cis* to N, and thus facilitating H-bond formation and stabilizing the structure (Fig. 6). Additionally, in this isomer the CH of the *N*-substituent is directed towards the center of the ring. The relatively low energy of these isomers confirms that the intramolecular hydrogen bond successfully competes with unfavorable steric interactions, e.g. with the steric strain between the bulky axial *N*-substituent and the equatorially disposed adjacent methyl unit. Although, the formation of structures different from stereoisomers **2b(A-D)** cannot be excluded, according to these results it is reasonable to assume that intramolecular hydrogen bonding is the major factor responsible for the non-stereoselective coordination. [32]

Finally, the DFT analysis of the possible isomers of complex [Pd(**2c**)Cl_2] predicts the formation of two isomers having axially disposed *N*-substituent (Fig. 7). These structures are again interconvertible through nitrogen- and ring inversion. Their similar stability in this case is due to the fact that the 2-hydroxyethyl group has less steric demand compared to the *N*-substituent of **2b**. As a result, the repulsion between the *N*-substituent and the equatorial methyl in **2c(B)** is not significant and both structures (**2c(A)** and **2c(B)**) are stabilized by hydrogen bonding. In other words, the formation of hydrogen bonds does not significantly influence the stereoselectivity of the coordination in [Pd(**2c**)Cl_2]. In contrast to this, the possibility of intramolecular hydrogen bonding in the solution phase of **2a** and **2b** having bulkier *N*-substituent, strongly affects the relative stability of the different chelate ring conformations.

In order to investigate the effect of the differences in the stereoselectivity of coordination on the catalytic performance we tested ligands **1a-c** in Pd-catalyzed asymmetric allylic alkylation reactions of the benchmark substrate diphenylallyl acetate using dimethyl malonate as a nucleophile precursor. The reactions were carried out in CH_2Cl_2 at a substrate/catalyst molar ratio of 100 at room temperature. Complete conversion could be achieved in each case after 1 h reaction time.

In the enantiodetermining step of Pd-catalyzed asymmetric allylic alkylation, the nucleophilic agent attacks one of the allylic termini of the corresponding Pd(II)-η^3-allyl intermediate to form Pd(0)-η^2-alkene complexes. Therefore, the stereoselective coordination of the ligand to the Pd(II)-center in the Pd(II)-η^3-allyl intermediate is crucial to achieve high enantioselectivity. Compounds **1a** and **1b** are expected to coordinate stereoselectively due to the absence of hydrogen acceptor chloro-ligands in the allyl complexes, that could change the coordination pattern of **1b**. Contrarily, the coordination of ligand **1c** with sterically less demanding *N*-substituent can lead to the formation of different chelate isomers. Indeed, the relatively low selectivity (58 %) achieved by using ligand **1c** is the result of the low stereoselectivity of its coordination. The best enantioselectivity, 96 %, could be obtained by ligand **1a**, while ligand **1b** provided the product with somewhat lower *ee* (90 %). It is important to underline that the catalysts modified by **1a** and **1b**,

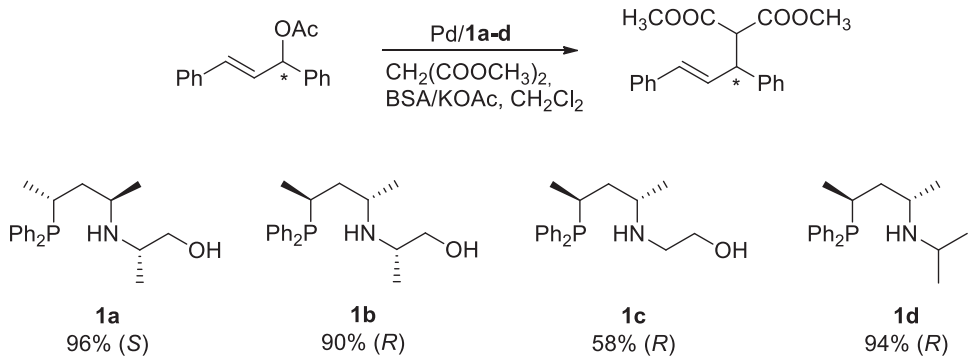

Fig. 8. Pd-catalyzed asymmetric allylic alkylation using ligands **1a-d.**

having opposite backbone chirality, yielded the product enantiomers with opposite configuration. It is also worth noting that the *N*-isopropyl analogue of **1b** (**1d**) provided the product (*R*)-malonate with 94 % *ee* under the same reaction conditions (Fig. 8). This fact emphasizes that it is the configuration of the pentane-2,4-diyl backbone that dictates the absolute configuration of the product. Additionally, it also corroborates the fact that the ligands prefer the same pentane-2,4-diyl based chelate conformation with axially disposed *N*-substituent in their intermediate η^3-diphenylallyl complexes as was found in the X-ray structures of **2a-b**.

However, as was reported by Moberg and coworkers, OH…Pd(0) type hydrogen bonds can stabilize the product Pd(0)-alkene complexes. [27] As the catalytic reaction proceeds towards the alkene-complex during the attack of the nucleophile, the formation of the hydrogen-bond between the OH and the metal may change the topology of the catalyst thus influencing the stereochemical outcome of the reaction. [28] It is therefore surmised that the difference in the selectivity of the catalysts containing ligands **1a** or **1b** might originate from this phenomenon. Although the role of hydrogen bonding cannot be unambiguously proved in the catalytic process, it is important to emphasize that ligand **1a** with hydroxyl substituent and properly tuned stereochemistry provided somewhat higher enantioselectivity than its unsubstituted analogue **1d**.

4. Conclusions

In conclusion, we have synthesized three novel chiral phosphine-aminoalcohol (P,N,OH) type chiral ligands **1a-c** having stereogenic nitrogen donoratom in order to investigate the effect of the OH-substituent on their coordination chemistry and catalytic properties. In the solid phase of complexes [Pd(**1a-b**)Cl_2] an intra- and an intermolecular hydrogen bond could be observed, respectively, between the OH-substituent of the chiral ligand and one of the Cl co-ligands of the metal. In the solution phase of [Pd(**1**)Cl_2] type complexes intramolecular hydrogen bonding appeared as a crucial factor in determining the stereoselectivity of the coordination. Additionally, the presence of the hydroxyl-substituent in the chiral ligand was shown to affect the enantioselectivity available in Pd-catalyzed allylic alkylation suggesting that the OH-group participates in hydrogen bonding during the catalytic cycle. It was shown that the introduction of the OH function with the properly tuned stereochemistry can be a useful design element that may improve catalytic performance. Our results also emphasize that apparently minor changes in the ligand structure can provide drastic differences in their coordination properties and catalytic features.

CRediT authorship contribution statement

Zsófia Császár: Methodology, Investigation. **Mária Guóth:** Investigation. **Evelin Farsang:** Investigation. **Attila C. Bényei:** Conceptualization, Writing – review & editing, Investigation. **József Bakos:** Writing – review & editing, Supervision, Conceptualization. **Gergely Farkas:** Writing – original draft, Supervision, Conceptualization.

Declaration of Competing Interest

The authors declare that they have no known competing financial interests or personal relationships that could have appeared to influence the work reported in this paper.

Data availability

No data was used for the research described in the article.

Acknowledgements

We thank Mr Béla Édes for skillful assistance in analytical measurements and synthetic experiments. The scientific program was supported by the project NKFIH K128074. This work has been implemented by the TKP2021-NKTA-21 project with the support provided by the Ministry for Innovation and Technology of Hungary from the National Research, Development and Innovation Fund, financed under the 2021 Thematic Excellence Programme funding scheme.

References

[1] P.J. Walsh, A.E. Lurain, Balsells, Use of achiral and meso ligands to convey asymmetry in enantioselective catalysis, J. Chem. Rev. 103 (2003) 3297–3344, https://doi.org/10.1021/cr0000630.
[2] K.A. Pelz, P.S. White, M.R. Gagné, Persistent *N*-chirality as the only source of asymmetry in nonracemic N_2PdCl_2 complexes, Organometallics 23 (2004) 3210–3217, https://doi.org/10.1021/om0498495.
[3] K.N. Gavrilov, A.I. Polosukhin, Chiral P, N-bidentate ligands in coordination chemistry and organic catalysis involving rhodium and palladium, Russ. Chem. Rev. 69 (2000) 661–682, https://doi.org/10.1070/RC2000v069n08ABEH000559.
[4] M.P. Carrol, P.J. Guiry, P, N ligands in asymmetric catalysis, Chem. Soc. Rev. 43 (2014) 819–833, https://doi.org/10.1039/C3CS60302D.
[5] A.M. Masdeu-Bultó, M. Diéguez, E. Martin, M. Gómez, Chiral thioether ligands: coordination chemistry and asymmetric catalysis, Coord. Chem. Rev. 242 (2003) 159–201, https://doi.org/10.1016/S0010-8545(03)00106-1.
[6] H. Pelissier, Chiral sulfur-containing ligands for asymmetric catalysis, Tetrahedron 63 (2007) 1297–1330, https://doi.org/10.1016/j.tet.2006.09.068.
[7] R.G. Arrayás, J.C. Carratero, Chiral thioether-based catalysts in asymmetric synthesis: recent advances, Chem. Commun. 47 (2011) 2207–2211, https://doi.org/10.1039/C0CC03978K.
[8] M. Coll, O. Pàmies, M. Diéguez, Highly versatile Pd–thioether–phosphite catalytic systems for asymmetric allylic alkylation, amination, and etherification reactions org, Lett. 16 (2014) 1892–1895, https://doi.org/10.1021/ol500758y.
[9] V. Schnitzler, G. Nonglaton, H. Roussière, C. Maillet, M. Evain, P. Janvier, B. Bujoli, M. Petit, Nitrogen-based chirality effects in novel mixed phosphorus/nitrogen ligands applied to palladium-catalyzed allylic substitutions, Organometallics 27 (2008) 5997–6004, https://doi.org/10.1021/om800498a.
[10] M. Coll, O. Pàmies, M. Diéguez, A modular furanoside thioether-phosphite/phosphinite/ phosphine ligand library for asymmetric iridium-catalyzed hydrogenation of minimally functionalized olefins: scope and limitations, Adv. Synth. Catal. 355 (2013) 143–160, https://doi.org/10.1002/adsc.201200711.
[11] Z. Császár, G. Farkas, A. Bényei, G. Lendvay, I. Tóth, J. Bakos, Stereoselective coordination: a six-membered P, N-chelate tailored for asymmetric allylic alkylation, Dalton Trans. 44 (2015) 16352–16360, https://doi.org/10.1039/C5DT02750K.

[12] G. Farkas, Z. Császár, K. Stágel, E. Nemes, S. Balogh, I. Tóth, A. Bényei, G. Lendvay, J. Bakos, Efficient stereochemical communication in phosphine-amine palladium-complexes: exploration of N-substituent effects in coordination chemistry and catalysis, J. Organomet. Chem. 846 (2017) 129–140, https://doi.org/10.1016/j.jorganchem.2017.04.033.

[13] B. Feng, X.-Y. Pu, Z.-C. Liu, W.-J. Xiao, J.-R. Chen, Highly enantioselective Pd-catalyzed indole allylic alkylation using binaphthyl-based phosphoramidite-thioether ligands, Org. Chem. Front. 3 (2016) 1246–1249, https://doi.org/10.1039/C6QO00227G.

[14] B. Lu, B. Feng, H. Ye, J.-R. Chen, W.-J. Xiao, Pd/phosphoramidite thioether complex-catalyzed asymmetric N-allylic alkylation of hydrazones with allylic acetates, Org. Lett. 20 (2018) 3473–3476, https://doi.org/10.1021/acs.orglett.8b01226.

[15] J. Margalef, O. Pàmies, M. Diéguez, Phosphite-thiother ligands derived from carbohydrates allow the enantioswitchable hydrogenation of cyclic β-enamides by using either Rh or Ir catalysts, Chem. Eur. J. 23 (2017) 813–822, https://doi.org/10.1002/chem.201604483.

[16] J. Margalef, X. Caldentey, E.A. Karlsson, M. Coll, J. Mazuela, O. Pàmies, M. Diéguez, M.A. Pericàs, A theoretically-guided optimization of a new family of modular P, S-ligands for iridium-catalyzed hydrogenation of minimally functionalized olefins, Chem. Eur J. 20 (2014) 12201–12214, https://doi.org/10.1002/chem.201402978.

[17] M. Biosca, J. Margalef, X. Caldentey, M. Besora, C. Rodríguez-Escrich, J. Saltó, X. C. Cambeiro, F. Maseras, O. Pàmies, M. Diéguez, M.A. Pericàs, Computationally guided design of a readily assembled phosphite-thioether ligand for a broad range of Pd-catalyzed asymmetric allylic substitutions, ACS Catal. 8 (2018) 3587–3601, https://doi.org/10.1021/acscatal.7b04192.

[18] J. Bayardon, S. Jugé, P-Chiral ligands, in: Phosphorus(III) Ligands in Homogeneous Catalysis (eds. Kamer, P.C.J.; van Leewen, P.W.N.M.), Wiley, Chichester, 2013, pp. 355–389.

[19] S. Lemouzy, L. Giordano, D. Hérault, G. Buono, Introducing chirality at phosphorus atoms: an update on the recent synthetic strategies for the preparation of optically pure P-stereogenic molecules, Eur. J. Org. Chem. 2020 (2020) 3351–3366, https://doi.org/10.1002/ejoc.202000406.

[20] D.A. Evans, K.R. Campos, J.S. Tedrow, F.E. Michael, M.R. Gagné, Application of chiral mixed phosphorus/sulfur ligands to palladium-catalyzed allylic substitutions, J. Am. Chem. Soc. 122 (33) (2000) 7905–7920, https://doi.org/10.1021/ja992543i.

[21] K.T. Mahmudov, M.N. Kopylovich, M.F.C.G., A.J.L. da Silva Pombeiro, (eds.), Noncovalent Interactions in Catalysis, 2019, The Royal Society of Chemistry, CPI Group (UK) Ltd, Croydon, CR0 4YY, UK.

[22] W.S. Knowles, W.C. Christopfel, K.E. Koenig, C.F. Hobbs, Studies of asymmetric homogeneous catalysts, Adv. Chem. Ser. 196 (1982) 325–336, https://doi.org/10.1021/ba-1982-0196.ch020.

[23] A. Börner, The effect of internal hydroxy groups in chiral diphosphane rhodium(I) catalysts on the asymmetric hydrogenation of functionalized olefins, Eur. J. Inorg. Chem. 2001 (2001) 327–337, https://doi.org/10.1002/1099-0682(200102)2001:2<327::AID-EJIC327>3.0.CO;2-A.

[24] T. Hayashi, A. Yamamoto, Y. Ito, E. Nishioka, H. Miura, K. Yanagi, Asymmetric synthesis catalyzed by chiral ferrocenylphosphine – transition-metal complexes. 8. Palladium-catalyzed asymmetric allylic amination, J. Am. Chem. Soc. 111 (1989) 6301–6311, https://doi.org/10.1021/ja00198a048.

[25] K. Nordström, E. Macedo, C. Moberg, Enantioselective allylic substitutions catalyzed by [(hydroxyalkyl)pyridinooxazoline]- and [(alkoxyalkyl) pyridinooxazoline]palladium complexes, J. Org. Chem. 62 (1997) 1604–1609, https://doi.org/10.1021/jo961490+.

[26] M. Svensson, U. Bremberg, K. Hallman, I. Csöregh, C. Moberg, (Hydroxyalkyl) pyridinooxazolines in palladium-catalyzed allylic substitutions. Conformational preferences of the ligand, Organometallics 18 (1999) 4900–4907, https://doi.org/10.1021/om990552u.

[27] K. Hallman, A. Frölander, T. Wondimagegn, M. Svensson, C. Moberg, OH–Pd(0) interaction as a stabilizing factor in palladium-catalyzed allylic alkylations, Proc. Natl. Acad. Sci. U. S. A 101 (2004) 5400–5404, https://doi.org/10.1073/pnas.0307084101.

[28] A. Frölander, S. Lutsenko, T. Privalov, C. Moberg, Conformational preferences and enantiodiscrimination of phosphino-4-(1-hydroxyalkyl)oxazoline−metal−olefin complexes resulting from an OH−metal hydrogen bond, J. Org. Chem. 70 (2005) 9882–9891, https://doi.org/10.1021/jo051610q.

[29] L. Yao, H. Nie, D. Zhang, L. Wang, Y. Zhang, W. Chen, Z. Li, X. Liu, S. Zhang, Chiral ferrocenyl N, N ligands with intramolecular hydrogen bonds for highly enantioselective allylic alkylations, ChemCatChem 10 (2018) 804–809, https://doi.org/10.1002/cctc.201701461.

[30] G. Farkas, Z. Császár, S. Balogh, I. Tóth, J. Bakos, Synthesis of hemilabile P, N-ligands with a pentane-2,4-diyl backbone, Tetrahedron Lett. 55 (2014) 4120–4122, https://doi.org/10.1016/j.tetlet.2014.05.091.

[31] G. Aullón, D. Bellamy, L. Brammer, E.A. Bruton, A. Guy Orpen, Metal-bound chlorine often accepts hydrogen bonds, Chem. Commun. (1998) 653–654, https://doi.org/10.1039/A709014E.

[32] The substitution of the OH-functionality in **2b(A)** and **2b(D)** by hydrogen atom leads to structures **2d(A)** and **2d(B)** (see in the Supplementary Information), respectively. The enthalpy difference between **2d(A)** and **2d(B)** is 21 kJ/mol, that is significantly higher than that between **2b(A)** and **2b(D)** (7 kJ/mol). This fact also emphasizes the stabilizing effect of the OH…Cl interaction in the original structure **2b(D)**.